THE JOURNAL OF PHYSICAL CHEMISTRY A

Article

pubs.acs.org/JPCA

Vibrationally Mediated Photodissociation of CH_3I [v_1 = 1] at 277.5 nm: The Vibrationally Adiabatic Process

Lili Hu, Zhimin Zhou, Changwu Dong, Lijuan Zhang, Yikui Du,* Min Cheng,* and Qihe Zhu

National Laboratory of Molecular Sciences, State Key Laboratory of Molecular Reaction Dynamics, Institute of Chemistry, Chinese Academy of Sciences, Beijing 100190, P. R. China

ABSTRACT: From the photofragment translational spectra of C−H symmetric stretch excited CH_3I [v_1 = 1, v_2 = 0] photodissociatioin at 277.5 nm, the vibrational distribution of photofragments CH_3 (v_1 = 0, v_2 = 0), (0,1), (1,0), (1,1) in the I* channel are measured to be 0.02, 0.02, 0.47, 0.25, and those of CH_3 (1,0), (1,1) in the I channel are 0.04, 0.05, respectively. It shows that most of the dissociated CH_3I [1,0] retain the C−H symmetric stretch vibration v_1 = 1 in the photofragments CH_3, and the vibrational distribution in umbrella bending mode is not seriously affected by the original C−H symmetric stretch excitation. The photodissociation of CH_3I [1,0] mainly follows the vibrationally adiabatic process. The original vibrational excitation [v_1 = 1] of CH_3I is quite like a spectator, and the intramolecular vibrational-energy redistribution (IVR) does not play obvious part during photodissociation.

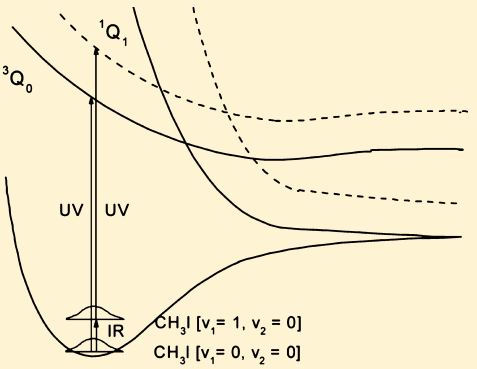

I. INTRODUCTION

The state-to-state reactions are widely investigated to give the important principles in chemical reaction dynamics. Most investigations on the photodissociation focus on the state population of the photofragments produced from the vibrational ground state reactant. In previous vibrationally mediated photodissociations, the dissociation bond is often selected to be vibrationally excited.[1,2] In the vibrationally mediated photodissociation of HOD molecules, the vibrationally excited bond can be selectively broken.[3−6] During the photodissociation of NH_3, the initial vibrational excitation of the symmetric or ansymmetric N−H stretch of NH_3 would influence the branching ratio of dissociation products differently.[7−9] The photodissociation of a molecule with vibrational excitation not on the dissociation bond has been studied relatively less. Dagdigian et al. have reported the different quantum yields Φ (Cl*) from the photodissociation of CH_3Cl with the CH stretch of different overtone excitation.[10]

CH_3I is a key molecule for elementary chemical reaction dynamics. Three repulsive potential energy surfaces (PESs), $^3Q_1$, $^3Q_0$, and $^1Q_1$, are involved in the photodissociation in the A band (210−350 nm). $^3Q_0$ correlates to the I* channel, while $^3Q_1$ and $^1Q_1$ correlate to the I channel.[11,12] There is a potential curve-crossing between $^1Q_1$ and $^3Q_0$.[13−15] The photodissociation of vibrational ground state CH_3I [v_1 = 0, v_2 = 0] has been studied frequently.[16−23] In the photodissociation of the ground state CH_3I [0,0] near the red edge of the A absorption band, the umbrella vibration (ν_2) of CH_3 is most easily excited in both I* and I channels, while relatively weak C−H symmetric stretch vibration (ν_1) of CH_3 excited only in the I channel.[16−21] Near the blue edge of the A band, the ν_1 mode of CH_3 fragments is intensely excited in both I and I* channels, coordinating with the excitation of the ν_2 mode.[16,22,23]

There are only a few studies on the photodissociation of the vibrationally excited CH_3I, mostly of the C−I stretch excited CH_3I from the hot band.[18,24] Near the red edge, the photodissociation of the hot-band CH_3I shows a larger photodissociation cross-section due to the enhanced Franck−Condon factor.[18]

In this work, we investigate the photofragment vibrational distribution of CH_3 at 277.5 nm from the C−H symmetric stretch excited CH_3I [v_1 = 1, v_2 = 0] prepared by a IR laser. The C−H symmetric stretch vibration (ν_1) is connected to photodissociation center C−I bond. It is very hard to imagine how much ν_1 original vibrational excitation would affect the photodissociation process. By detecting CH_3 fragments of different vibrational states from parent molecules CH_3I [0,0] and CH_3I [1,0], the influence can be investigated experimentally.

II. EXPERIMENTAL SETUP

The experimental apparatus is shown in Figure 1 and has been described previously.[18] The carrier gas Ar at 1 atm is bubbled through the liquid CH_3I sample (Sinopharm, Ltd., 99%) at room temperature to form the gas mixture, which expands supersonically from the pulsed valve into the source chamber. Three lasers cross the molecule beam at the same position. The IR laser from a OPO/OPA pumped by a Nd:YAG laser (Continuum Surelite EX) is tuned at 2969.3 cm^{-1} to excite CH_3I molecules to v_1 = 1 state. The line width of the IR laser is about 2−3 cm^{-1}. The photodissociation UV laser from a dye laser (Sirah) pumped by a Nd:YAG laser (Spectra-Physics,

Received: February 5, 2013
Revised: April 15, 2013
Published: April 24, 2013

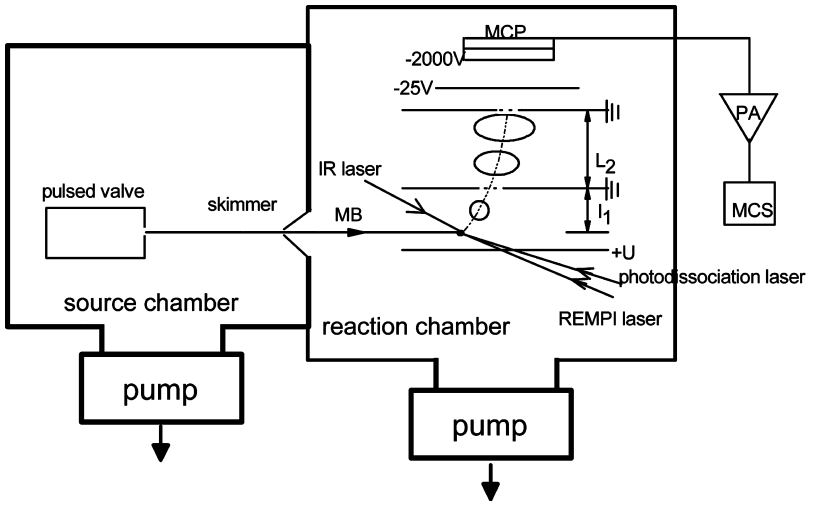

Figure 1. Schematic diagram of the experimental apparatus.

Quanta-Ray 230) is set at 277.5 nm to dissociate CH_3I via $X \rightarrow {}^3Q_0$. The detection UV laser (from another dye laser) is tuned to (2 + 1) REMPI wavelength of the state-selected CH_3 fragments: 333.5 nm for ground state CH_3 (0,0), 333.9 nm for CH_3 (1,0), and 329.4 nm for CH_3 (0,1) and CH_3 (1,1). The IR laser arrives about 40 ns before the photodissociation laser, and the ionization laser arrives 4 ns later than the photodissociation laser. The polarization of the IR and of the photodissociation laser are parallel to the detection axis, while the polarization of the detection laser is perpendicular. The IR laser energy is kept constant at 8 mJ/pulse. The energy of the two UV lasers are less than 0.2 mJ/pulse.

III. EXPERIMENTAL RESULTS

The photofragment translational spectra (PTS) of CH_3I photodissociation at 277.5 nm have been measured by detecting I and I* separately also with IR off and IR on. Integrating the PTS, we get $\sigma^{off}(I) \approx \sigma^{on}(I)$ and $\sigma^{off}(I^*) \approx \sigma^{on}(I^*)$. No appreciable difference has been found between σ^{on} and σ^{off} both in the I channel and the in I* channel. From $\sigma^{off} = \sigma_{[0,0]}$ and $\sigma^{on} = (1 - p_{exc})\sigma_{[0,0]} + p_{exc}\sigma_{[1,0]}$ for the I and I* channels, where p_{exc} is the IR excitation fraction of CH_3I [0,0] $\rightarrow$ CH_3I [1, 0] (given in the next section), we have deduced the ratio of the photodissociation cross section $\sigma_{[1,0]}/\sigma_{[0,0]} = [\sigma_{[1,0]}(I) + \sigma_{[1,0]}(I^*)]/[\sigma_{[0,0]}(I) + \sigma_{[0,0]}(I^*)] \approx 1 \pm 0.17$, which will be used in the following data analysis.

From the conservation of energy, we have

$$E_{int}(CH_3I) + h\nu = D_0(H_3C{-}I) + E_{SO} + E_{int}(CH_3) + E_t$$

where $E_{int}(CH_3I) \approx E_v(CH_3I)$ and $E_{int}(CH_3) \approx E_v(CH_3)$ for a C_{3v} molecule. The spin−orbit coupling energy of iodine $E_{SO} = 0$ for the I channel and $E_{SO} = 0.943$ eV for the I* channel. The peaks in the PTS can be assigned to the appropriate reaction subchannels, according to the translational energy E_t of photofragments calculated from the above energy equation.

a. The PTS at 277.5 nm from Detecting the CH_3 (0,0) Fragment. PTS at 277.5 nm from REMPI detecting CH_3 (0,0) at 333.5 nm are shown in Figure 2.

Peak A CH_3I [0, 0] $\rightarrow$ CH_3 (0, 0) + I*,
denoted as [0, 0] $\rightarrow$ (0, 0)*

Peak C CH_3I [1, 0] $\rightarrow$ CH_3 (0, 0) + I*,
denoted as [1, 0] $\rightarrow$ (0, 0)*

Peak B CH_3I [0, 0] $\rightarrow$ CH_3 (0, 0) + I,
denoted as [0, 0] $\rightarrow$ (0, 0)

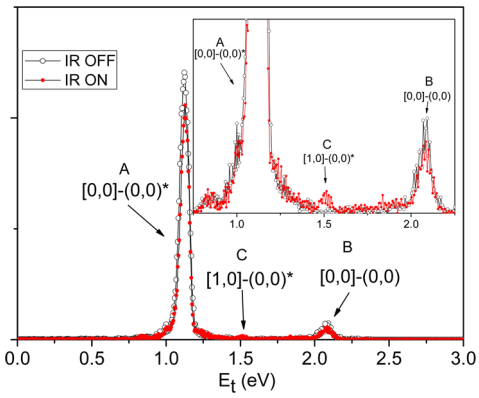

Figure 2. The PTS at 277.5 nm from REMPI detecting CH_3 (0,0) at 333.5 nm. The inset is the enlarged PTS.

When IR is turned from OFF to ON, the two peaks A and B have a decrease due to the IR excitation of CH_3I [0,0] to CH_3I [1,0]. The fraction p_{exc} of IR excitation [0,0] $\xrightarrow{IR}$ [1,0] can be calculated from the decrease of the high peak A,

$$p_{exc} = \frac{[1,0]^{on}}{[0,0]^{off}} = \frac{[0,0]^{off} - [0,0]^{on}}{[0,0]^{off}} = \frac{(0,0)^{off} - (0,0)^{on}}{(0,0)^{off}} = \frac{S_A^{off} - S_A^{on}}{S_A^{off}} = 0.18$$

where S_A^{off} is the area of peak A for IR OFF; S_A^{on} is the area of peak A for IR ON.

In Figure 2, from peak C, compared with peak A^{off}, the fraction $p_{[1,0]-(0,0)^*} = [(0,0)^*/\sum(\nu_1,\nu_2)]^{on}_{[1,0]}$ of CH_3 (0,0)* from CH_3I [1,0] can be calculated.

From the area ratio $S_C^{on}/S_A^{off} = (p_{exc}\sigma_{[1,0]}/\sigma_{[0,0]}) \times (p_{[1,0]-(0,0)^*}/p_{[0,0]-(0,0)^*})$, then

dx.doi.org/10.1021/jp401310g | J. Phys. Chem. A 2013, 117, 4352−4357

$$p_{[1,0]-(0,0)^*} = p_{[0,0]-(0,0)^*} \times \frac{S_C^{on}}{S_A^{off}} \times \frac{\sigma_{[0,0]}}{p_{exc} \times \sigma_{[1,0]}}$$
$$= 0.40 \times 0.009 \times \frac{1}{0.18} = 0.02$$

where S_C^{on} is the area of peak C (IR ON), $\sigma_{[0,0]}$ is the photodissociation cross section of CH_3I [0,0], $\sigma_{[1,0]}$ is the photodissociation cross section of CH_3I [1,0], and $p_{[0,0]-(0,0)^*} = [(0,0)^*/\sum(\nu_1,\nu_2)]_{[0,0]} = 0.40$ is the known fraction of CH_3 (0,0)* fragment from CH_3I [0,0] at 277.5 nm as given in Table 1.

Table 1. The Measured Vibrational Distribution of CH_3 Photofragment from Photodissociation of CH_3I[1,0] at 277.5 nm, Compared with Published CH_3 Vibrational Distribution from Photodissociation of CH_3I[0,0]

state−state dissociation			
CH_3I [0,0]	fraction[a]	CH_3I [1,0]	fraction
[0,0]→(1,1)*	$p_{[0,0]-(1,1)^*} = 0$	[1,0]→(1,1)*	$p_{[1,0]-(1,1)^*} = 0.25$
[0,0]→(1,0)*	$p_{[0,0]-(1,0)^*} = 0$	[1,0]→(1,0)*	$p_{[1,0]-(1,0)^*} = 0.47$
[0,0]→(0,2)*	$p_{[0,0]-(0,2)^*} = 0.03$		
[0,0]→(0,1)*	$p_{[0,0]-(0,1)^*} = 0.16$	[1,0]→(0,1)*	$p_{[1,0]-(0,1)^*} = 0.02$
[0,0]→(0,0)*	$p_{[0,0]-(0,0)^*} = 0.40$	[1,0]→(0,0)*	$p_{[1,0]-(0,0)^*} = 0.02$
[0,0]→(1,1)	$p_{[0,0]-(1,1)} = 0.03$	[1,0]→(1,1)	$p_{[1,0]-(1,1)} = 0.05$
[0,0]→(1,0)	$p_{[0,0]-(1,0)} = 0.04$	[1,0]→(1,0)	$p_{[1,0]-(1,0)} = 0.04$
[0,0]→(0,3)	$p_{[0,0]-(0,3)} = 0.05$		
[0,0]→(0,2)	$p_{[0,0]-(0,2)} = 0.09$		
[0,0]→(0,1)	$p_{[0,0]-(0,1)} = 0.11$	[1,0]→(0,1)	$p_{[1,0]-(0,1)} = 0$
[0,0]→(0,0)	$p_{[0,0]-(0,0)} = 0.08$	[1,0]→(0,0)	$p_{[1,0]-(0,0)} = 0$

[a]From ref 18.

b. The PTS at 277.5 nm from Detecting the CH_3 (1,0) Fragment. PTS at 277.5 nm, from REMPI detecting CH_3 (1,0) at 333.9 nm, are shown in Figure 3. CH_3 (0,0) fragments are also weakly ionized.

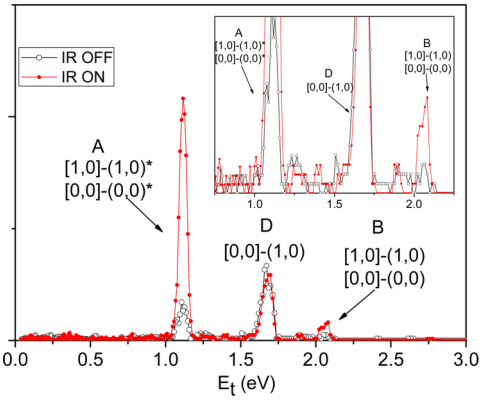

Figure 3. The PTS at 277.5 nm from REMPI detecting CH_3 (1,0) at 333.9 nm.

Peak A CH_3I [1, 0] → CH_3 (1, 0) + I*,
denoted as [1, 0] → (1, 0)*

CH_3I [0, 0] → CH_3 (0, 0) + I*,
denoted as [0, 0] → (0, 0)* weak

Peak D CH_3I [0, 0] → CH_3 (1, 0) + I,
denoted as [0, 0] → (1, 0)

Peak B CH_3I [1, 0] → CH_3 (1, 0) + I,
denoted as [1, 0] → (1, 0)

CH_3I [0, 0] → CH_3 (0, 0) + I,
denoted as [0, 0] → (0, 0) weak

In Figure 3, when IR OFF is turned to IR ON, the peak A and B increase intensely due to IR excitation [0,0] → [1,0], and then [1,0] → (1,0)* and [1,0] → (1,0). From the increase of peak A, compared with peak D^{off}, the fraction $p_{[1,0]-(1,0)^*}$ of CH_3 (1,0)* from CH_3I [1,0] can be calculated.

From $[S_A^{on} - (1 - p_{exc})S_A^{off}]/S_D^{off} = (p_{exc}\sigma_{[1,0]}/\sigma_{[0,0]}) \times (p_{[1,0]-(1,0)^*}/p_{[0,0]-(1,0)})$, then

$$p_{[1,0]-(1,0)^*} = p_{[0,0]-(1,0)} \times \frac{S_A^{on} - (1 - p_{exc}) \times S_A^{off}}{S_D^{off}}$$
$$\times \frac{\sigma_{[0,0]}}{p_{exc} \times \sigma_{[1,0]}} = 0.04 \times 2.13 \times \frac{1}{0.18} = 0.47$$

Similarly, from the increase of peak B, compared with peak D^{off}, the fraction $p_{[1,0]-(1,0)}$ of CH_3 (1,0) from CH_3I [1,0] can be calculated.

From $[S_B^{on} - (1 - p_{exc})S_B^{off}]/S_D^{off} = (p_{exc}\sigma_{[1,0]}/\sigma_{[0,0]}) \times (p_{[1,0]-(1,0)}/p_{[0,0]-(1,0)})$, then

$$p_{[1,0]-(1,0)} = p_{[0,0]-(1,0)} \times \frac{S_B^{on} - (1 - p_{exc}) \times S_B^{off}}{S_D^{off}}$$
$$\times \frac{\sigma_{[0,0]}}{p_{exc} \times \sigma_{[1,0]}} = 0.04 \times 0.16 \times \frac{1}{0.18} = 0.04$$

c. The PTS at 277.5 nm from Detecting Both CH_3 (0,1) and CH_3 (1,1) Fragments. PTS at 277.5 nm from REMPI detecting both CH_3 (0,1) and CH_3 (1,1) at 329.4 nm are shown in Figure 4.

Peak A′ CH_3I [0, 0] → CH_3 (0, 1) + I*,
denoted as [0, 0] → (0, 1)*

CH_3I [1, 0] → CH_3 (1, 1) + I*,
denoted as [1, 0] → (1, 1)*

Peak E CH_3I [1, 0] → CH_3 (0, 1) + I*,
denoted as [1, 0] → (0, 1)*

Peak F CH_3I [0, 0] → CH_3 (1, 1) + I,
denoted as [0, 0] → (1, 1)

Peak B′ CH_3I [0, 0] → CH_3 (0, 1) + I,
denoted as [0, 0] → (0, 1)

CH_3I [1, 0] → CH_3 (1, 1) + I,
denoted as [1, 0] → (1, 1)

dx.doi.org/10.1021/jp401310g | J. Phys. Chem. A 2013, 117, 4352−4357

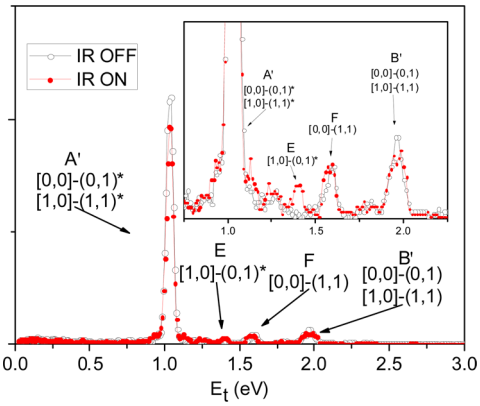

Figure 4. The PTS at 277.5 nm from REMPI detecting CH_3 (0,1) and CH_3 (1,1) at 329.4 nm.

From peak E, compared with peak A'^{off}, the fraction $p_{[1,0]-(0,1)*}$ of CH_3 (0,1)* from CH_3I [1,0] can be calculated.

From $S_E^{on}/S_{A'}^{off} = (p_{exc}\sigma_{[1,0]}/\sigma_{[0,0]}) \times (p_{[1,0]-(0,1)*}/p_{[0,0]-(0,1)*})$, then

$$p_{[1,0]-(0,1)*} = p_{[0,0]-(0,1)*} \times \frac{S_E^{on}}{S_{A'}^{off}} \times \frac{\sigma_{[0,0]}}{p_{exc} \times \sigma_{[1,0]}}$$

$$= 0.16 \times 0.024 \times \frac{1}{0.18} = 0.02$$

The peak A′ has a decrease from IR OFF to IR ON due to the decrease of the ground state CH_3I [0,0] as in Figure 2. However, the decrease of the A′ peak is only 12%, apparently less than p_{exc} = 18% of peak A in Figure 2. The extra 6% signal comes from [1,0] → (1,1)*. From the extra signal of peak A′, compared with peak F^{off}, the fraction $p_{[1,0]-(1,1)*}$ of CH_3 (1,1)* from CH_3I [1,0] can be calculated.

From $[S_{A'}^{on} - (1 - p_{exc}) \times S_{A'}^{off}]/S_F^{off} = (p_{exc}\sigma_{[1,0]}/\sigma_{[0,0]}) \times (p_{[1,0]-(1,1)*}/p_{[0,0]-(1,1)})$, then

$$p_{[1,0]-(1,1)*} = p_{[0,0]-(1,1)} \times \frac{S_{A'}^{on} - (1 - p_{exc}) \times S_{A'}^{off}}{S_F^{off}}$$

$$\times \frac{\sigma_{[0,0]}}{p_{exc} \times \sigma_{[1,0]}} = 0.03 \times 1.48 \times \frac{1}{0.18} = 0.25$$

Similarly, the peak B′ has a decrease of only 2%, which is also less than 18%. The extra 16% signal comes from [1,0] → (1,1). From the extra signal of peak B′, compared with peak F^{off}, the fraction $p_{[1,0]-(1,1)}$ of CH_3 (1, 1) from CH_3I [1, 0] can be calculated.

From $[S_{B'}^{on} - (1 - p_{exc}) \times S_{B'}^{off}]/S_F^{off} = (p_{exc}\sigma_{[1,0]}/\sigma_{[0,0]}) \times (p_{[1,0]-(1,1)}/p_{[0,0]-(1,1)})$, then

$$p_{[1,0]-(1,1)} = p_{[0,0]-(1,1)} \times \frac{S_{B'}^{on} - (1 - p_{exc}) \times S_{B'}^{off}}{S_F^{off}}$$

$$\times \frac{\sigma_{[0,0]}}{p_{exc} \times \sigma_{[1,0]}} = 0.03 \times 0.30 \times \frac{1}{0.18} = 0.05$$

All the experimental vibrational distributions are summarized in Table 1. The uncertainty of each measured fraction $p_{[1,0]-(\nu_1,\nu_2)}$ is estimated to be about ±20%.

IV. DISCUSSION

From the experimental measurements of Figures 2−4, for the 277.5 nm photodissociation of the C−H symmetric stretch excited CH_3I [1,0], it is summarized in Table 1 that 81% of CH_3 photofragments retain the original ν_1 = 1 vibration, and only 4% of CH_3 have lost the ν_1 = 1 vibration. The 81% of photofragment $CH_3(1,\nu_2)$ from CH_3I [1,0] photodissociation at 277.5 nm is much higher than ∼7% of CH_3 $(1,\nu_2)$ from the CH_3I [0,0] photodissociation at 277 nm. The 81% of CH_3 $(1,\nu_2)$ is even much higher than that from CH_3I [0,0] at the wavelength of 248 or 240 nm (with more available energy than from CH_3I [1,0] at 277.5 nm).[16,17,25] The rest of the fractions of about 15% CH_3 from CH_3I [1,0] are mainly due to the unmeasured vibrational states of CH_3. By comparing the vibrational distributions of CH_3 from CH_3I [1,0] and CH_3I [0,0] as shown in Table 1, it is reasonable to deduce that the important unmeasured CH_3 fragments are CH_3 (1,2), (1,3) and (1,2)*, which all are ν_1 = 1 retained states. After estimation of these states, the percentage of v_1 = 1 retained $CH_3(1,\nu_2)$ would be more than 90% from CH_3I [1,0].

Comparing the vibrational distributions of photofragments from CH_3I [1,0] and from CH_3I [0,0] as shown in Table 1, the main fractions from [1,0] $p_{[1,0]-(1,x)}$ resemble the main fractions from [0,0] $p_{[0,0]-(0,x)}$ both in the I* channel and in the I channel, presented in the same color in Figure 5. For the main

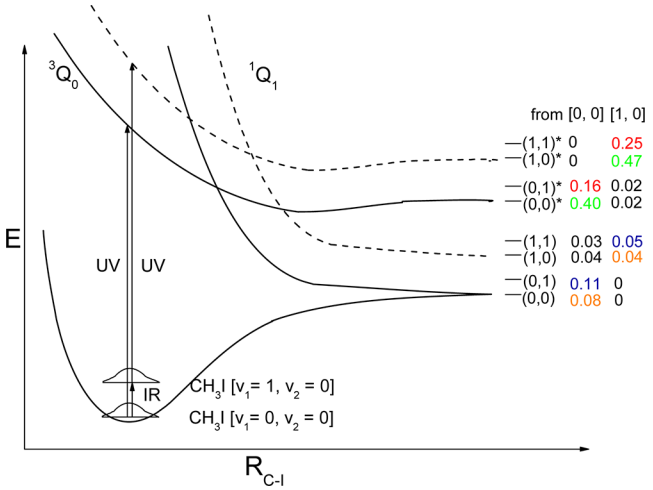

Figure 5. The schematic diagram of CH_3I photodissociation and a summary of the experimental results. The dash lines are ν_1 = 1 vibrationally adiabatic potential energy curves. The spectator effect is shown: the fractions with the same color belong to the similar excitation in ν_2 mode.

fractions, (1,1)*/(1,0)* = 0.25/0.47 = 0.53 from [1,0] resembles (0,1)*/(0,0)* = 0.16/0.40 = 0.40 from [0,0] in the I* channel, and (1,1)/(1,0) = 0.05/0.04 = 1.3 from [1,0] resembles (0,1)/(0,0) = 0.11/0.08 = 1.4 from [0,0] in the I channel. The original ν_1 = 1 excitation in CH_3I is mostly retained in the CH_3 fragments, and does not seriously influence the ν_2 vibrational excitation ratios of CH_3, showing that the original ν_1 = 1 vibration is quite like a spectator during photodissociation.

From the measured distributions of CH_3 (ν_1, ν_2) in Table 1, the I* branching fraction (≈ 0.76) from [1,0] is relatively greater than ≈0.59 from [0,0]. According to the Landau−Zener equation, the curve crossing probability is closely related to the coupling of the electronic states ($^3Q_0$ and $^1Q_1$) and the relative

dx.doi.org/10.1021/jp401310g | J. Phys. Chem. A 2013, 117, 4352−4357

velocity dR_{C-I}/dt in the crossing region. The photodissociation path and crossing region of [1,0] on the nine-dimensional PESs are different from those of [0,0], so a different coupling term between PESs is reasonable. Also in the situation of [1,0], more available energy may lead to a higher velocity in the crossing region and a higher I* branching fraction. There is at least 4% dissociating CH_3I [1,0] transferring the original $\nu_1 = 1$ vibrational energy into translational energy, detected only in the I* channel. It is reasonable to have a higher I* branching fraction from [1,0] than from [0,0]. However, this higher I* branching fraction from [1,0] has not been found in PTS of detecting I* and I, mainly due to the low $P_{exc} = 0.18$ of [1,0].

For vibrationally excited parent molecules, the complexity of photodissociation dynamics would increase greatly due to the coupling between different degrees of freedom (DOF). The intramolecular vibrational-energy redistribution (IVR) might occur from the original vibration excitation to other vibrational modes during the photodissociation. It is reported in the photodissociation of C−H symmetric stretch excited $BaFCH_3$, when the C−H symmetric stretch vibration energy is transferred to the C−F bond through IVR, it leads to dissociation on the stronger C−F bond instead of on the weaker Ba−F bond.[26] However, in the present experimental results, the IVR seems to be not effective in the photodissociation of CH_3I [1, 0] at 277.5 nm. The original ν_1 vibrational excitation in the CH_3 moiety is found to be mostly retained and does not effectively influence the relative distribution of the umbrella (ν_2) mode as shown in Table 1.

The experimental results of photodissociation of CH_3I [1,0] can be explained as follows. The CH_3I [1,0] will be dominantly retained at the $\nu_1 = 1$ vibration of the C−H symmetric stretch DOF when being excited from the X state to the $^3Q_0$ state, due to the similar topology of $^3Q_0$ and X in the ν_1 DOF.[14] The experimental results of this work also imply that in the photodissociation process of about 100 fs,[27] the wavepacket on the $^3Q_0$ PES does not dissipate appreciably in the C−H symmetric stretch DOF. There are two factors that may ensure the dominant CH_3I [1,0] → CH_3 (1,0), (1,1). One is the relatively small energy difference of 34 cm^{-1} between the ν_1 frequency of the parent molecule CH_3I and the "ν_1 frequency" of the photofragment CH_3. Another is that the vibrational period (~11 fs) of the $\nu_1 = 1$ vibration is much shorter than the dissociation duration (~100 fs). The dissociating CH_3I is easy to accommodate itself to the PESs in the C−H symmetric stretch DOF. As shown in Figure 5, the vibrationally adiabatic potential curves[28,29] seem to be suitable to describe the photodissociation of CH_3I [1,0] at 277.5 nm reasonably.

V. CONCLUSION

In the experimental vibrational distribution of the photofragment CH_3 from the photodissociation of C−H symmetric stretch excited CH_3I [1,0] at 277.5 nm, more than 90% of the CH_3I [1,0] retain the C−H symmetric stretch vibration ($\nu_1 = 1$) in the CH_3 photofragments. Excluding the extra $\nu_1 = 1$ vibration, the umbrella ν_2 vibrational distribution of CH_3 from CH_3I [1,0] resembles the ν_2 vibrational distribution of CH_3 from CH_3I [0,0], as shown in Table 1. It implies that the dissociating CH_3I [1,0] mostly remain in $\nu_1 = 1$ of the C−H symmetric stretch DOF. The photodissociation of CH_3I [1,0] mainly follows the vibrationally adiabatic potential curves.

AUTHOR INFORMATION

Corresponding Author

*E-mail: chengmin@iccas.ac.cn (M.C.); ydu@iccas.ac.cn (Y.D.).

Notes

The authors declare no competing financial interest.

ACKNOWLEDGMENTS

This work is supported by the National Natural Science Foundation of China under Grants No. 21203207 and 21173236.

REFERENCES

(1) Sato, H. Photodissociation of simple molecules in the gas phase. *Chem. Rev.* **2001**, *101*, 2687−2725.

(2) Crim, F. F. Molecular reaction dynamics across the phases: Similarities and Differences. *Faraday Discuss.* **2012**, *157*, 9−26.

(3) Vanderwal, R. L.; Scott, J. L.; Crim, F. F.; Weide, K.; Schinke, R. An experimental and theoretical study of the bond selected photodissociation of HOD. *J. Chem. Phys.* **1991**, *94*, 3548−3555.

(4) Bar, I.; Cohen, Y.; David, D.; Arusi-Parpar, T.; Rosenwaks, S.; Valentini, J. J. Mode-selective bond fission: Comparison between the photodissociation of HOD (0, 0, 1) and HOD (1, 0, 0). *J. Chem. Phys.* **1991**, *95*, 3341−3346.

(5) Vander Wal, R. L.; Scott, J. L.; Crim, F. F. Selectively breaking the O−H bond in HOD. *J. Chem. Phys.* **1990**, *92*, 803−805.

(6) Adhikari, S.; Deshpande, S.; Sarma, M.; Kurkal, V.; Mishra, M. K. Selective control of photodissociation in deutereted water molecule HOD. *Radiat. Phys. Chem.* **2006**, *75*, 2106−2118.

(7) Hause, M. L.; Yoon, Y. H.; Crim, F. F. Vibrationally mediated photodissociation of ammonia: The influence of N−H stretching vibrations on passage through conical intersections. *J. Chem. Phys.* **2006**, *125*, 174309.

(8) Bach, A.; Hutchison, J. M.; Holiday, R. J.; Crim, F. F. Competition between adiabatic and nonadiabatic pathways in the photodissociation of vibrationally excited ammonia. *J. Phys. Chem. A* **2003**, *107*, 10490−10496.

(9) Bach, A.; Hutchison, J. M.; Holiday, R. J.; Crim, F. F. Photodissociation of vibrationally excited ammonia: Rotational excitation in the NH_2 product. *J. Chem. Phys.* **2003**, *118*, 7144−7145.

(10) Tao, C.; Dagdigian, P. J. Vibrationally mediated photodissociation of CH_3Cl: The $\nu = 3$ and 4 CH stretch overtone levels. *Chem. Phys. Lett.* **2001**, *350*, 63−70.

(11) Gedanken, A.; Rowe, M. D. Magnetic circular dichroism spectra of methyl halides. Resolution of the n → σ^* continuum. *Chem. Phys. Lett.* **1975**, *34*, 39−43.

(12) Mulliken, R. S. Intensities in Molecular Electronic Spectra X. Calculations on Mixed-Halogen, Hydrogen Halide, Alkyl Halide, and Hydroxyl Spectra. *J. Chem. Phys.* **1940**, *8*, 382−395.

(13) Alekseyev, A. B.; Liebermann, H.-P.; Buenker, R. An ab initio study of the CH_3I photodissociation. I. Potential energy surfaces. *J. Chem. Phys.* **2007**, *126*, 234102.

(14) Amatatsu, Y.; Yabushita, S.; Morokuma, K. Full nine-dimensional ab initio potential energy surfaces and trajectory studies of A-band photodissociation dynamics: CH_3I^* → CH_3 + I, CH_3 + I^*, and CD_3I^* → CD_3 + I, CD_3 + I^*. *J. Chem. Phys.* **1996**, *104*, 9783−9794.

(15) Ajitha, D.; Wierzbowska, M.; Lindh, R.; Malmqvist, P. A. Spin-orbit ab initio study of alkyl halide dissociation via electronic curve crossing. *J. Chem. Phys.* **2004**, *121*, 5761−5766.

(16) Eppink, A. T. J. B.; Parker, D. H. Energy partitioning following photodissociation of methyl iodide in the A band: A velocity mapping study. *J. Chem. Phys.* **1999**, *110*, 832−844.

(17) Eppink, A. T. J. B.; Parker, D. H. Methyl iodide A-band decomposition study by photofragment velocity imaging. *J. Chem. Phys.* **1998**, *109*, 4758−4767.

(18) Cheng, M.; Yu, Z.; Hu, L.; Yu, D.; Dong, C.; Du, Y.; Zhu, Q. Vibrationally resolved photofragment translational spectroscopy of CH_3I from 277 to 304 nm with increasing effect of the hot band. *J. Phys. Chem. A* **2011**, *115*, 1153−1160.
(19) Li, G. S.; Shin, Y. K.; Hwang, H. J. State-to-state reaction dynamics of CH_3I photodissociation at 304 nm. *J. Phys. Chem. A* **2005**, *109*, 9226−9231.
(20) Li, G. S.; Hwang, H. J.; Jung, H. C. High resolution kinetic energy by long time-delayed core-sampling photofragment translational spectroscopy. *Rev. Sci. Instrum.* **2005**, *76*, 023105.
(21) Aguirre, F.; Pratt, S. T. Photodissociation of vibrationally hot CH_3 and CF_3. *J. Chem. Phys.* **2005**, *122*, 234303.
(22) Hu, L. L.; Zhou, Z. M.; Dong, C. W.; Zhang, L. J.; Du, Y. K.; Cheng, M.; Zhu, Q. H. Photofragment translational spectroscopy of CH_3I at 225 nm-with the high excitation of the symmetric stretch vibration of CH_3 fragment. *J. Chem. Phys.* **2012**, *137*, 144302.
(23) González, M. G.; Rodríguez, J. D.; Rubio-Lago, L.; García-Vela, A.; Bañares, L. Slice imaging and wave packet study of the photodissociation of CH_3I in the blue edge of the A-band: Evidence of reverse $^3Q_0 \leftarrow {}^1Q_1$ non-adiabatic dynamics. *Phys. Chem. Chem. Phys.* **2011**, *13*, 16404−16415.
(24) Rubio-Lago, L.; García-Vela, A.; Arregui, A.; Amaral, G. A.; Bañares, L. The photodissociation of CH_3I in the red edge of the A-band: Comparison between slice imaging experiments and multisurface wave packet calculations. *J. Chem. Phys.* **2009**, *131*, 174309.
(25) Zhu, Q.; Continetti, R. E.; Lee, Y. T. et al.. Unpublished results.
(26) Lippert, H.; Manz, J.; Oppel, M.; Paramonov, G. K.; Radloff, W.; Ritze, H. H.; Stert, V. Control of breaking strong versus weak bonds of $BaFCH_3$ by femtosecond IR plus VIS laser pulses: Theory and experiment. *Phys. Chem. Chem. Phys.* **2004**, *6*, 4283−4295.
(27) de Nalda, R.; Durá, J.; García-Vela, A.; Izquierdo, J. G.; González-Vázquez, J.; Bañares, L. A detailed experimental and theoretical study of the femtosecond A-band photodissociation of CH_3I. *J. Chem. Phys.* **2008**, *128*, 244309.
(28) Schinke, R. *Photodissociation Dynamics: Spectroscopy and Fragmentation of Small Polytomic Molecules*; Cambridge University Press: Cambridge, U.K., 1993.
(29) Sage, A. G.; Oliver, T. A. A.; Murdock, D.; Crow, M. B.; Ritchie, G. A. D.; Harvey, J. N.; Ashfold, M. N. R. $n\sigma^*$ and $\pi\sigma^*$ excited states in aryl halide photochemistry: A comprehensive study of the UV photodissociation dynamics of iodobenzene. *Phys. Chem. Chem. Phys.* **2011**, *13*, 8075−8093.